Iraqi Journal of Physics, 2018 *Vol.16, No.39, PP. 135-151*

DOI: 10.20723/ijp.16.39.135-151

Ag-SiO_2 nanoparticales prepared by Sol-Gel methods for antibacterial effect

M.Th.AL-Azawi[1], Ch.H.Mohammed[1], Sabah Mahdi Hadi [2]

[1]Department of Physics, College of Science, University of Baghdad

[2]Department of Biology, College of Science, University of Baghdad

E-mail: ghuson.hamed@yahoo.com

Abstract

Sol-gel method was use to prepare Ag-SiO_2 nanoparticles. Crystal structure of the nanocomposite was investigated by means of X-ray diffraction patterns while the color intensity was evaluated by spectrophotometry. The morphology analysis using atomic force microscopy showed that the average grain sizes were in range (68.96-75.81 nm) for all samples. The characterization of Ag-SiO_2 nanoparticles were investigated by using Scanning Electron Microscopy (SEM). Ag-SiO_2 NPs are highly stable and have significant effect on both Gram positive and negative bacteria. Antibacterial properties of the nanocomposite were tested with the use of *Staphylococcus aureus* (*S. aureus*) *and Escherichia coli* (*E. coli*) bacteria. The results have shown antibacterial effect of the Ag-SiO_2 prepared as nanogel and nanopowder states, while the Ag-SiO_2 nanopowder showed the highest capability against *S. aureus*. Both methods of biofilm showed an inhibition effect for Ag-SiO_2 NPs, the synthetic Ag-SiO_2 NPs showed highest inhibition effect on Gram positive bacteria *S. aureus* by using the biofilm microtiter method.

Key words

Sol-gel, Silica-silver, antibacterial, characterized, biofilm and antimicrobial activity.

Article info.

Received: Sep. 2018
Accepted: Oct. 2018
Published: Dec. 2018

تحضير فضة-سليكا النانوية باستخدام طريقة السول جل لتاثيرها المضاد للجراثيم

مريم ثامر العزاوي[1]، غصون حميد محمد[1]، صباح مهدي هادي[2]

[1]قسم الفيزياء، كلية العلوم، جامعة بغداد

[2]قسم علوم الحياة، كلية العلوم، جامعة بغداد

الخلاصة

تم استخدام طريقة سول-جل لتحضير فضة-سليكا النانوية. وتم فحص البنية البلورية لمركب النانو عن طريق أنماط حيود الأشعة السينية بينما تم تقييم شدة اللون بواسطة القياس الطيفي. وأظهر التحليل المورفولوجي باستخدام مجهر القوة الذرية أن معدل الحجم الحبيبي في مدى (68.96-75.81) نانومتر لجميع العينات. تم توصيف جسيمات فضة-سليكا النانوية باستخدام تحليل المجهر الالكتروني الماسح. تتميز جسيمات فضة-سليكا النانوية بأنها مستقرة بشكل كبير ولها تأثير كبير على كل من البكتيريا الموجبة والسالبة الجرام. تم اختبار خصائص مضادة للجراثيم للمركب النانو مع استخدام المكورات العنقودية الذهبية وبكتيريا الاشريكية القولونية. وقد أظهرت النتائج تأثير مضاد للبكتريا للفضة-سليكا والتي أعدت في الحالتين السائل والمسحوق، بينما المسحوق فضة-سليكا نانوي اظهر أعلى قدرة ضد المكورات العنقودية الذهبية. طريقة الغشاء الحيوي اظهرت تأثير تثبيطي لجسيمات فضة-سليكا النانوية، حيث اظهرت جسيمات سليكا-فضه النانوية اعلى تأثير تثبيطي على البكتيريا موجبة الجرام المكورات العنقودية الذهبي باستخدام طريقة العيار الميكروي للغشاء الحيوي.

Introduction

The sol-gel has several advantages such as high purity, ultra-homogeneity and low synthesis temperature [1]. The sol-gel process has been touted as an exciting and potentially useful technique for the preparation of high performance materials. The advantage of this process include the purity of reagents, the control of the degree of homogeneity of mixing of the precursors, the potential control of the phase evolution and structure, and the opportunity for fabrication of materials into useful non-traditional shapes (fibers, thin films, spheres, optical elements, patterned surfaces, etc.) [2].

Silver doped silica sol-gel finds the application possibility in many areas, like sensors and batteries or by the preparation of photosensitive [3]. But also result in an extremely high hydrophilicity of hybrid particles [4]. The Ag-SiO_2 composites have a large surface area and high adsorption properties; thus, the bacteria could be adsorbing by Ag-SiO_2 nanocomposites easily [5]. Meanwhile, silica nanospheres have high surface, high adsorption properties; reactivity and considered as a supporting material according to the previous study [6]. The antibacterial results demonstrate that the Ag-SiO_2 composites have better antibacterial properties compared to the silver NPs, by preventing the aggregation and oxidation [7] of silver NPs and by continuously releasing silver ions [8].

It is a chemical synthesis of nanomaterials that involves the evolution of inorganic networks through the formation of a colloidal suspension (sol) and gelation of the sol to form a network in a continuous liquid phase (gel) [9]. The sol-gel process is a method for producing solid materials from small molecules, it is based on inorganic polymerization reactions and the size of the sol particles depends on the solution composition, pH and temperature. The sol-gel process includes five steps [10];

- **Prepare precursor:** choose proper alkoxide and design sol gel path.
- **Hydrolysis and condensation:** generate sol.
- **Gelation:** generate wet gel.
- **Aging and drying:** generate solid gel.
- **Annealing:** remove organics, ROH and other residuals.

Materials and methods

Preparation of hot aqueous extract of *Thuja orientalis*

The leaves of *T. orientalis* were collected from the University of Baghdad gardens. Plant parts were washed several times by using tap water then by distilled water (D.W) to remove all dirt then dried at room temperature. After that, the samples were grinded to powder by using electrical grinder (Kahiscal, USA); 10 gm of dried powder was added to 100 ml of dionized water (diH_2O). Then, boiling for 10 min in order to homogenization by using magnetic stirrer (Gallenkamp, England) for 4h then the mixture was filtered with filter paper Wattman No.1. The extract was centrifuged at 5000 rpm for 15 min and storied at 4 $^{\circ}$C until use [11].

Preparation of silver nanoparticles by using green method

Silver nanoparticles were synthesized by added 45 ml of 1×10^{-3} M of $AgNO_3$ (Merck, > 99.5) solution for bio reduction process in a flask placed in a water bath with continuous stirring until the temperature stabilized at 60 $^{\circ}$C. 5 ml of aqueous leaf extract was added, after 16 min a change in the mixture color was occurred after a few seconds from pale yellow to yellow brown then dark brown color, which an indicator for the formation of silver nanoparticles [12].

Preparation of Ag-SiO_2 nanocomposite

The sol-gel process includes steps for all samples prepared in a sol-gel method before annealing and switch to powder as shown in Fig. 1 [10];

(1) **Hydrolysis condensation:** generate sol.
(2) **Gelation:** generate wet gel.
(3) **Aging and drying:** generate solid gel.

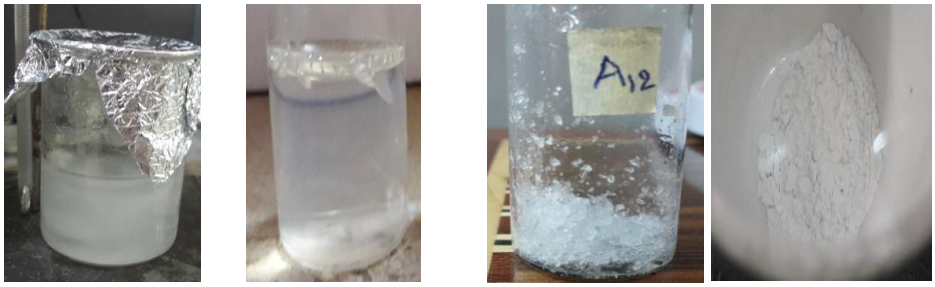

(1) (2) (3)

Fig. 1: Steps of nanopowder synthesis for all samples prepared in a sol-gel method. (1) Hydrolysis and condensation for precursor to produce sol. (2) The sol gelation and wet gel production. (3) Aging to produce solid gel and drying powder to obtain nanoparticle material.

Chemical synthesis by sol-gel method of Ag-SiO_2 nanopowder with 10^{-3} M $AgNO_3$

Two and a half (2.5) ml of Tetraethyl orthosilicate (TEOS) mixed with 22.5 ml ethanol by using magnetic stirred (Gallenkamp, England) for 30 min, then 13 ml of distilled water (D.W) was added, 0.12 ml HNO_3 and 12 ml of 10^{-3} M $AgNO_3$, were added and put under intense stirring at room temperature. In order to assure that the reaction was completed, the solution was gentle stirred during 4 hrs. Finally, the product was dried at room temperature one week gelation. The obtained bulk samples were grinded into fine powders and annealed in air at 600 $^{\circ}$C for 1h, we got a pale yellow powder.

Chemical synthesis by sol-gel method of Ag-SiO_2 nanopowder with silver NPs that prepared by using hot aqueous extract of *T. orientalis*.

Silver NPs were fabricated according to the green method. Two and a half (2.5) ml of Tetraethyl orthosilicate (TEOS) and 22.5 ml ethanol (EtOH) mixed by using magnetic stirred for 30 min, after that 13 ml of distilled water (D.W), 0.12 ml HNO_3 and 12 ml of Ag NPs, were added and put under intense stirring at room temperature. In order to assure that the reaction was completed, the solution was gentle stirred during 4 hrs. Finally, the product was dried at room temperature one week gelation. The obtained bulk samples were grinded into fine powders and annealed in air at 600 $^{\circ}$C for 1h, we got a white powder.

Synthesis of Ag-SiO_2 NPs with molar ratio ($AgNO_3$: TEOS= 0.12).

Ag-SiO_2 nanocomposite powders were prepared by using sol-gel method. The precursors consisted of Tetraethyl orthosilicate (TEOS, Si $(OC_2H_5)_4$, Merck), ethanol (C_2H_5OH, Merck), distilled water, nitric acid (HNO_3, Merck) and silver nitrate ($AgNO_3$, Merck), by using the molar ratios 1: 13: 12: 0.2: 0.12 respectively [13]. In the first step, $AgNO_3$ and distilled water was mixing then stirred for 30 min at room temperature to form solution – A. In another beaker, TEOS and ethanol was also mixing for 30

minutes to obtain solution - B. Then, solution - B was slowly poured into solution – A under stirring. After 30 min stirring, HNO_3 is added to the mixture. The final solution was continuously stirred for 4 hrs at room temperature and then placed into sealed polypropylene container. The gelation was exposed to the air, then after one week the obtained bulk sample was grinded into fine powder. This powder was annealed in air at 600 $^{\circ}$C for 1h. The resulting powder was like the mustard color.

Synthesis of Ag-SiO_2 NPs with molar ratio ($AgNO_3$: TEOS= 0.24).

SiO_2 containing small addition of silver was prepared when sol method has the following molar ratios: TEOS: ethanol: D.W: HNO_3: $AgNO_3$ = 1: 13: 12: 0.2: 0.24. The compounds were mixed at room temperature for 90 min and after adding silver nitrate for the next 30 min, after that they were placed into sealed polypropylene containers. The gelation was exposed to the air for one week then dried in the drying oven (30 min, 60 $^{\circ}$C) [13]. The obtained bulk sample was grinded into fine white powder. This powder was annealed in air at 600 $^{\circ}$C for 1h. The resulting powder color was brown.

Nanocomposite characterization:

X-ray diffraction measurements

In order to study the structural properties, the crystalline structure is examined by X-ray diffractions using a (Philips PW)1840 X-ray diffract meter system which records the intensity as a function of Bragg's angle. The source of radiation was Cu(kα) with wavelength =1.5406Å, the current was 30mA and the voltage was 40 kV. The scanning angle 2θ was varied in the range of (0-60) degree with speed of 5 deg/min.

Atomic Force Microscopy (AFM)

The surface morphology, particle size distribution of Ag-SiO_2NPs sample was analyzed by using atomic force microscopy (AFM), (SPM, Model AA3000), tip NSC35/AIBS from Angstrom Advanced Inc. (USA).

Scanning Electron Microscopy (SEM)

SEM (Hitachi FE-SEM model S-4160) was used to examine the surface topography of the prepared powders with a resolution down to a few nanometers.

UV-VIS spectroscopy

The optic absorption spectrum was used to study the optical properties of the synthesized Ag-SiO_2 nanoparticles. UV-Visible spectrophotometer (UV-Vis) refers to absorption spectroscopy in the ultraviolet-visible range directly affects the perceived color of the Ag, SiO_2 and Ag-SiO_2 NPs colloidal. In this region of the electromagnetic spectrum, molecules undergo electronic transitions. The test samples have been done by using UV-Vis type UV Metertech, SP-8001 spectrophotometer to measure the transmittance and absorption of NPs solutions samples in the range (200-1100) nm. All spectra have been measured at room temperature in a glass slides (1×1) cm^2 to samples were prepared by droplets of NPs placed on slides, and then dried at room temperature. The output data of wavelength, absorption were used in a computer program to deduce the absorbance spectrum.

Determination of antimicrobial activity by agar well diffusion

E. coli and S. aureus bacteria were obtained from the Central Environment Laboratory in Biology Department, College of Science/University of Baghdad.

Antimicrobial activity for the different synthesized silver-silica nanoparticles was determined against the pathogenic bacteria isolates (*S. aureus and E. coli*) by using modified Kirby-Bauer agar well diffusion method. In brief, bacterial culture was prepared by spreading of bacterial suspension (0.5×10^8 CFU/mL of each test organism) on solid Muller Hinton Agar. The wells (6 and 8 mm) were made in each of these plates by using a sterile micropipette tips for nanogel and nanopowder plate (compact or compressed powder) respectively. The wells in each plate loaded with 50µL of nanoparticles suspension (nanogel) and 0.05 gm for nanopowder. After incubation at 37 °C for 24hrs, the size of the inhibition zone around each well measured (Joa et al., 2015) [14].

Biofilm production by using a microtiter plate method

Biofilm formation assays were performed using 96- well microtiter plate, based on the protocol by Goh, S. *et al* (2013) [15], with slight modifications. *E. coli* and *S. aureus* bacteria were cultured in tryptone soya broth (TSB) for 18-24 hrs and the resulting culture was adjusted to 0.5 McFarland. All the wells of microtiter plate was loaded with 100µl of TS broth with 100 µl of nanoparticles solution while the control filled only broth to check sterility, then the plate was incubated at 37 °C for 24h. Each nanoparticles solution was tested triplicate. The microbial planktonic was removed by upset the plate over a waste tray then 0.1% w/v crystal violet solution was added to each well and left for 10 min at room temperature. The dye was removed by submerging the plate in a water tray, then was inverted and left in air to dry. The wells were treated with 95% v/v ethanol for 10 min to solubilize the dye. Optical density (OD) was measured at 630 nm [16].

Results and discussion

Structural propertization

X-ray diffraction patterns of powders annealed at 600 °C for 1h are revealed in Fig. 2. There are no peaks characterized for silver crystal phase are present at temperatures below 500 °C. After exposure to heat-treatment at 600 °C, the peaks will appear for all Ag-SiO_2 composites samples which have two Bragg peaks. It could be assigned to the (111) and (200) planes of silver crystals with Face Centered Cubic (F.C.C) phase, agree well with (I. K. Suh et al., 1988) [17], that means Ag NPs were successfully loaded onto the surface of the SiO_2 nanospheres. From the figure it released that a broad peak in the diffraction angle range of (2θ=15-30˚) and centered at 23˚ attributed to the amorphous structure for SiO_2 NPs, without any defined peaks due to the existing of crystalline structure, these results were agreed with (M. M. D. Lu et al., 2015) [18].

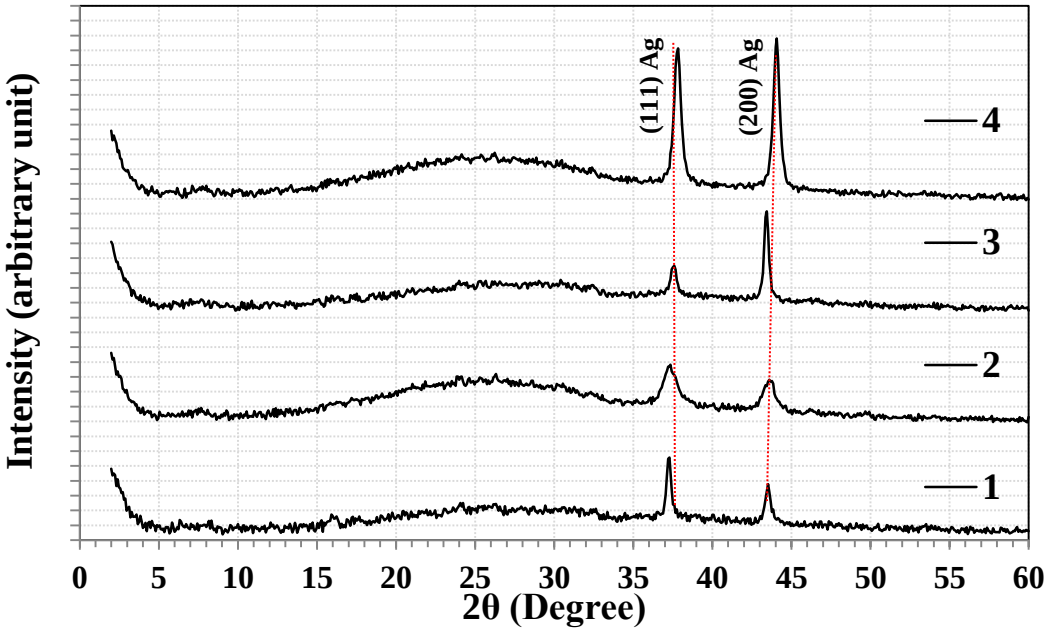

Fig. 2: XRD patterns of the Ag-SiO_2 nanopowders. 1) Ag-SiO_2 nanopowder that synthesize by using sol-gel method with 10^{-3} M $AgNO_3$. 2) Ag-SiO_2 nanopowder produced by using sol-gel method with silver NPs prepared by using hot aqueous extract of T. orientalis. 3) Ag-SiO_2 nanopowder synthesize by using sol-gel method with molar ratio $AgNO_3$: TEOS= 0.12. 4) Ag-SiO_2 nanopowder synthesize by using sol-gel method with molar ratio $AgNO_3$: TEOS= 0.24.

The calculated lattice parameter a=4.1660 Å, as well as the interplanar distances (d_{111} =2.4113Å, d_{200} =2.0779Å), (d_{111} =2.4074Å, d_{200} =2.0742Å), (d_{111} =2.3939Å, d_{200} =2.0824Å) and (d_{111} =2.3781Å, d_{200} =2.0536Å) agree well with the reported ones [19]. By using these reflections, the Scherrer formula, and a Gaussian distribution for the diffracted radiation intensity, In order to obtain a more accurate value of the average diameter of the NPs. The well-known Scherrer formula can be rewritten as [20]:

$$D = \frac{K'\lambda}{\beta' \cos\theta}$$

where D is mean crystallite size, β' is the width of the peak at half maximum intensity of a specific phase in radians, λ is the wavelength of incident rays, θ is the center diffraction angle of the peak in radian. The mean crystallite size for silver nanoparticles was evaluated to be 9.71 and 23.29 nm for all samples. Table 1 presents the structure parameters obtain for X-Ray diffraction result for Ag-SiO_2 NPs.

Table 1 reveals that average crystallite size decreases with increasing concentration for samples prepared without precursors dilution (TEOS and $AgNO_3$) for Ag-SiO_2 nanopowder synthesize by using sol-gel method with molar ratio AgNO3:TEOS= 0.24 as shown in Table 2 which gives the average crystalline size for the all Ag-SiO_2 NPs obtained for X-Ray diffraction results.

Table 1: Structural parameters of Ag-SiO_2 nanopowders NPs. 1) Ag-SiO_2 nanopowder that synthesize using sol-gel method with 10^{-3} M $AgNO_3$. 2) Ag-SiO_2 nanopowder produced by using sol-gel method with silver NPs prepared using hot aqueous extract of T. orientalis. 3) Ag-SiO_2 nanopowder synthesize using sol-gel method with molar ratio $AgNO_3$: TEOS= 0.12. 4) Ag-SiO_2 nanopowder synthesize using sol-gel method with molar ratio $AgNO_3$: TEOS= 0.24.

Samples	2θ (Deg.)	FWHM (Deg.)	d_{hkl} Exp.(Å)	D (nm)	hkl	d_{hkl} Std.(Å)	Phase	Card No.
1	37.2600	0.3530	2.4113	23.8	(111)	2.4052	Cub.Ag	96-901-3053
	43.5200	0.3750	2.0779	22.8	(200)	2.0830	Cub.Ag	96-901-3053
2	37.3218	0.9630	2.4074	8.7	(111)	2.4052	Cub.Ag	96-901-3053
	43.6000	0.8000	2.0742	10.7	(200)	2.0830	Cub.Ag	96-901-3053
3	37.5400	0.4210	2.3939	19.9	(111)	2.4052	Cub.Ag	96-901-3053
	43.4200	0.3240	2.0824	26.4	(200)	2.0830	Cub.Ag	96-901-3053
4	37.8000	0.4900	2.3781	17.1	(111)	2.4052	Cub.Ag	96-901-3053
	44.0600	0.4700	2.0536	18.2	(200)	2.0830	Cub.Ag	96-901-3053

Table 2: The average crystalline size for all nanopowder samples. 1) Ag-SiO_2 nanopowder that synthesize using sol-gel method with 10^{-3} M $AgNO_3$. 2) Ag-SiO_2 nanopowder produced using sol-gel method with silver NPs prepared using hot aqueous extract of T. orientalis. 3) Ag-SiO_2 nanopowder synthesize using sol-gel method with molar ratio $AgNO_3$: TEOS= 0.12. 4) Ag-SiO_2 nanopowder synthesize using sol-gel method with molar ratio $AgNO_3$: TEOS= 0.24.

Samples	Average crystalline size (nm)
1	23.29
2	9.71
3	23.17
4	17.69

Atomic Force Microscopy (AFM) measurement

The surface morphology was been investigated by using images of AFM which produces topological images of surface at very high magnification. Images of AFM are widely known, providing a useful tool for unambiguously describing the size and distribution of nanoparticle size. Fig. 3 show 2D and 3D images of Ag-SiO_2 NPs synthesis by using sol-gel method with 10^{-3} M $AgNO_3$.

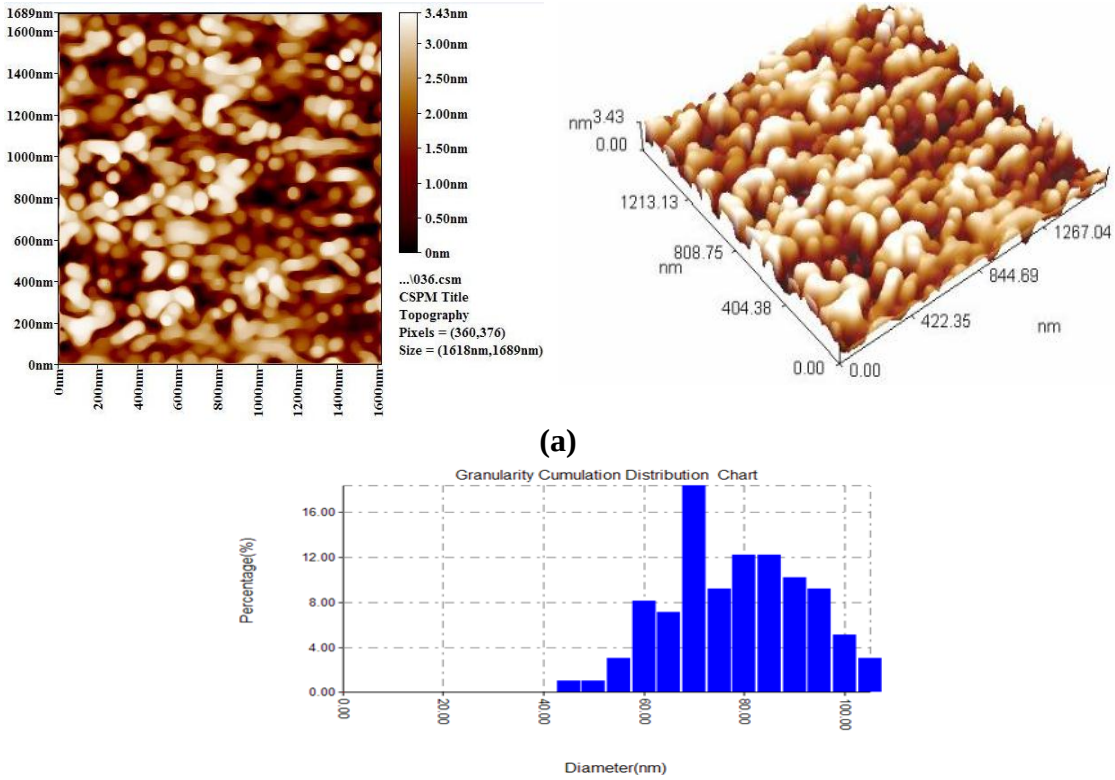

Fig. 3: (a) 3D& 2D AFM images of Ag-SiO_2 NPs that synthesize using sol-gel method with 10^{-3} M $AgNO_3$. (b) Granularity distribution of Ag-SiO_2 NPs that synthesize using sol-gel method with 10^{-3} M $AgNO_3$.

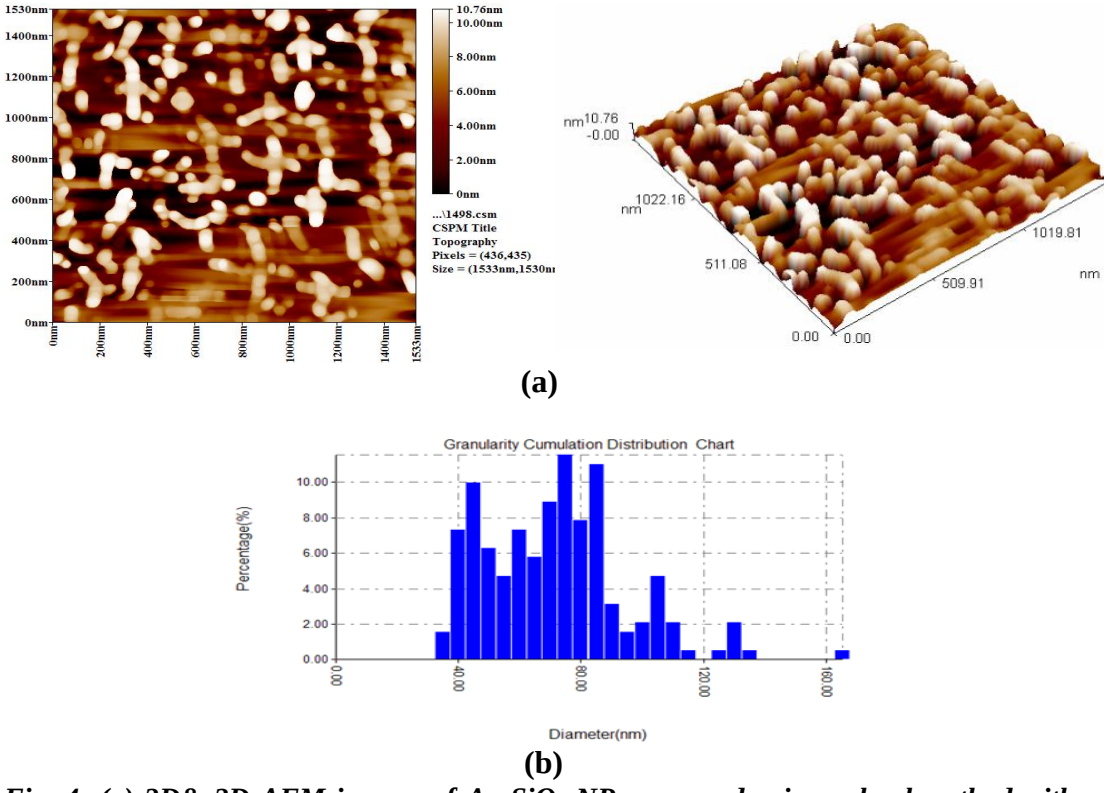

Fig. 4: (a) 3D& 2D AFM images of Ag-SiO_2 NPs prepared using sol-gel method with molar ratio ($AgNO_3$: TEOS = 0.24). (b) Granularity distribution of Ag-SiO_2 NPs prepared using sol-gel method with molar ratio ($AgNO_3$: TEOS = 0.24).

It is found that average grain size was 75.81 nm and 74.09 nm for samples synthesized by used 10^{-3} M $AgNO_3$ and Ag NPs synthesized by using hot aqueous extract of *T. orientalis* respectively. The average grain size decreases with addition that of Ag NPs in advance for specimen synthesized by using hot aqueous extract of *T. orientalis*. While, the average grain size decreases with increasing of concentration for sample synthesized by using sol-gel method with molar ratio ($AgNO_3$: TEOS = 0.24) as shown in Table 3. This result was good agreement with the results obtained from XRD measurements.

Table 3: The average grain sizes of Ag-SiO_2 NPs. 1) Ag-SiO_2 NPs that synthesize by using sol-gel method with 10^{-3} M $AgNO_3$. 2) Ag-SiO_2 NPs produced using sol-gel method with silver NPs prepared using hot aqueous extract of T. orientalis. 3) Ag-SiO_2 NPs synthesize using sol-gel method with molar ratio $AgNO_3$: TEOS= 0.12. 4) Ag-SiO_2 NPs synthesize using sol-gel method with molar ratio $AgNO_3$: TEOS= 0.24.

Samples	Average grain size (nm)
1	75.81
2	74.09
3	73.47
4	68.96

SEM analysis of Ag-SiO_2 NPs

The morphological features of Ag-SiO_2 nanopowder that chemical synthesize using sol-gel method with 10^{-3} M $AgNO_3$ (sample 1) was studied by SEM analysis shown in Fig.5. It is observed from image an existence of large masses with fine particles and aggregates with some and these particles are distinguishable from each other with a heterogeneous structure.

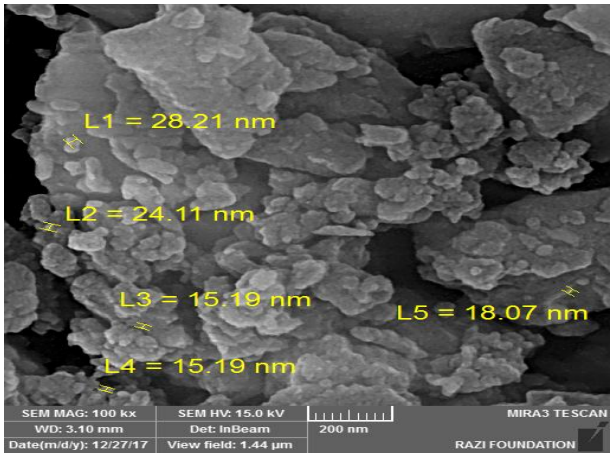

Fig. 5: SEM analysis for Ag-SiO_2 nanopowder that synthesize using sol-gel method with 10^{-3} M $AgNO_3$.

The analysis of the SEM for Ag-SiO_2 nanopowder chemical synthesize using sol-gel method with Ag NPs that prepared by using hot aqueous extract of *T. orientalis* in Fig. 6 shows a very high conglomerate level and the particles are indistinguishable with contact particles as well as have some uneven edges. We also note particles with a perfect spherical shape of up to 400 nm, possibly due to SiO_2 NPs.

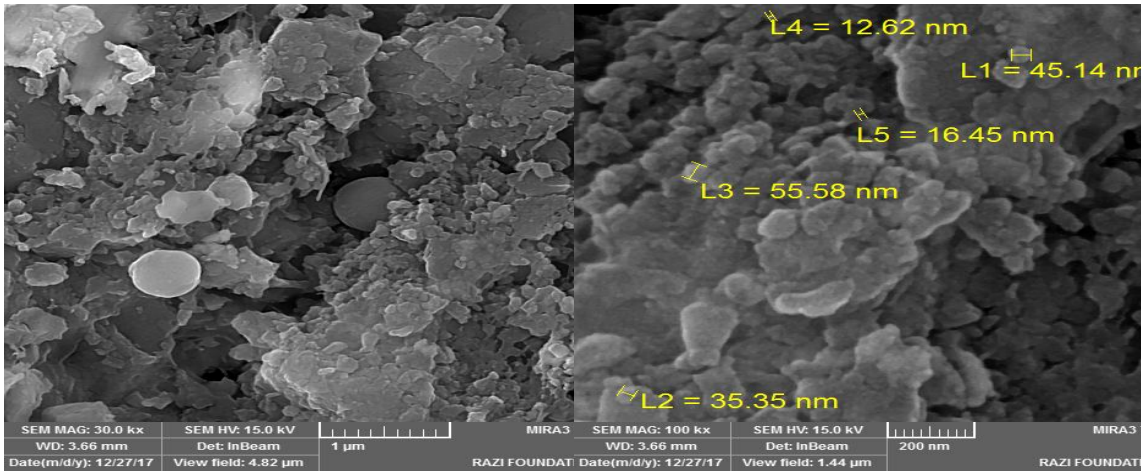

Fig. 6: SEM analysis for Ag-SiO_2 nanopowder produced using sol-gel method with silver NPs that prepared using hot aqueous extract of T. orientalis.

It can be observe the crystals with sharp edges as obtained in Fig. 7 of SEM analysis for Ag-SiO_2 nanopowder chemical synthesis by using sol-gel method with molar ratio ($AgNO_3$: TEOS = 0.12). The pure Ag NPs were nearly uniform spherical shapes and very small particles in evidently dispersed without large agglomerates. More addition of Ag to SiO_2 caused the agglomerates of grains due to the grain growth events.

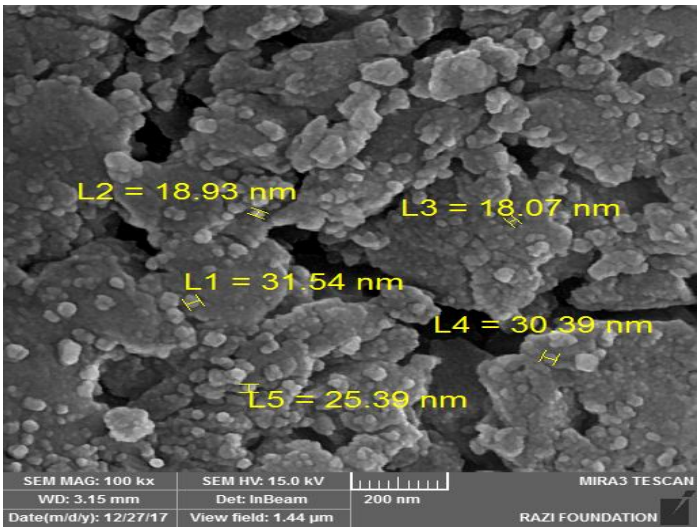

Fig. 7: SEM analysis for Ag-SiO_2 nanopowder prepared using sol-gel method with molar ratio ($AgNO_3$: TEOS = 0.12).

Fig. 8 shows that of Ag-SiO_2 nanopowder prepared by using sol-gel method and using molar ratio ($AgNO_3$: TEOS = 0.24) was taking a part of the surface a level of a high conglomerate with particles of large blocks.

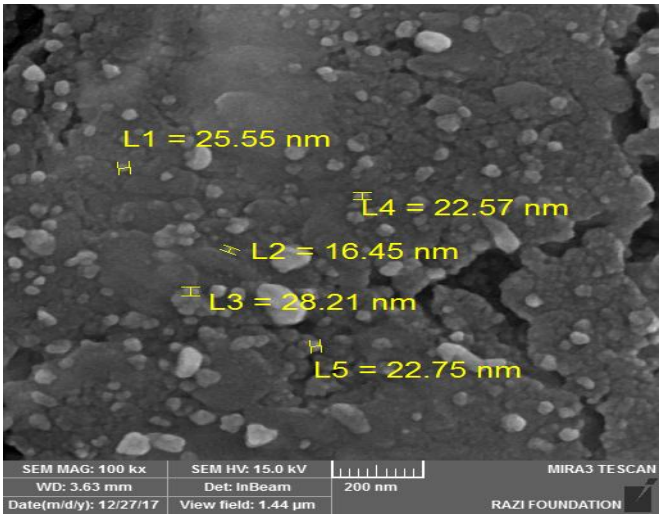

Fig. 8: SEM analysis for Ag-SiO_2 nanopowder prepared using sol-gel method with molar ratio ($AgNO_3$: TEOS = 0.24).

A SEM image of the Ag-SiO_2 nanopowder heat-treated at 600°C is presented in Figs. 5-8. Showing a relatively homogenous distribution of Ag spherical particles throughout the amorphous SiO_2 network. In the studies of a very large number of images for Ag-SiO_2 systems, the particle sizes range between 20.154-33.028 nm. This value correlates with that obtained from XRD data. Table 4 presents the particle size of Ag-SiO_2 nanopowder.

Table 4: The average particle sizes of Ag-SiO_2 nanopowder. 1) Ag-SiO_2 nanopowder that synthesize using sol-gel method with 10^{-3} M $AgNO_3$. 2) Ag-SiO_2 nanopowder produced using sol-gel method with silver NPs prepared by using hot aqueous extract of T. orientalis. 3) Ag-SiO_2 nanopowder synthesize using sol-gel method with molar ratio $AgNO_3$: TEOS= 0.12. 4) Ag-SiO_2 nanopowder synthesize using sol-gel method with molar ratio $AgNO_3$: TEOS= 0.24.

Samples	Average grain size (nm)
1	20.154
2	33.028
3	24.864
4	23.106

The results of Table 4 shows that the particle size decreases with increasing the concentration of the samples that synthesized by using sol-gel method with molar ratio ($AgNO_3$: TEOS= 0.24, 0.24). These results have good agreement with the results obtained from XRD and AFM measurements. We conclude from that smaller sized Ag-SiO_2 NPs have many positive attributes, such as good chemical stability and biofilm inhibition, which would make them suitable for many practical applications.

UV-Visible spectrum analysis of Ag-SiO_2 nanoparticles

The UV-Vis absorption spectrum of the chemical synthesized Ag-SiO_2 NPs has been recorded to measure their absorbance of material as a function of wavelength shown in Fig 9. The UV-Vis absorption spectra of both

samples 2 and 3 show two distinct absorption bands located around (350, 425) nm and (217, 400) nm. The peak at 350 nm and 217 is assigned to SiO_2-Ag ion complex or Ag ion clusters embedded in silica matrix [21]. Similar result was reported by Li et al. [22] where the appearance of the 350 nm and 217 was assigned to Ag cluster formation. The appearance of UV-Vis peak at 425 nm and 400 is due to the surface plasmon resonance (SPR) absorption of AgNPs [23]. The UV-Vis spectra suggested the presence of both ionic Ag and AgNPs in the silica matrix. While both the samples 1and 4 show only one distinct absorption bands located around 360 nm and 423 nm. We conclude that the absorption peaks are due to Ag NPs, not the presence of SiO_2, where the absorption peak at 400 nm represents the Ag NPs spherical and the blue shift indicates a decrease in the size of the nanoparticles while red shifting indicates the change of NPs shape from spherical to oval.

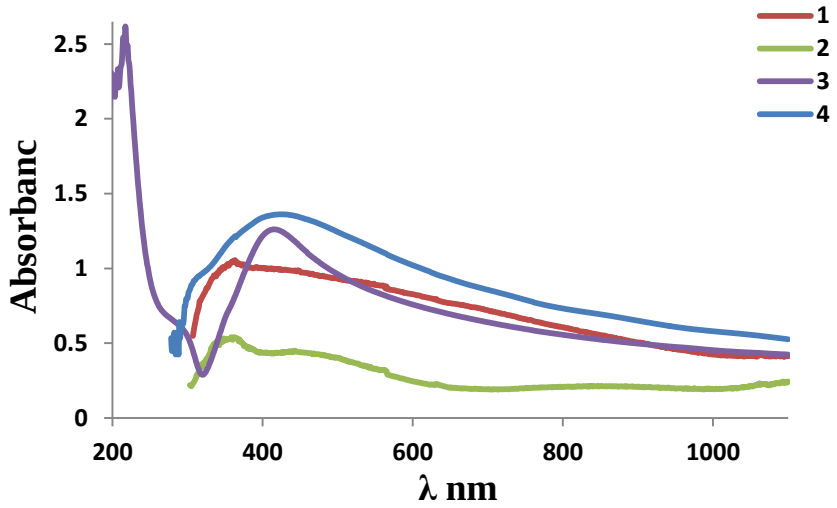

Fig. 9: UV-Vis absorbance spectra of Ag-SiO_2 NPs. 1) Ag-SiO_2 NPs that synthesize by using sol-gel method with 10^{-3} M $AgNO_3$. 2) Ag-SiO_2 NPs produced using sol-gel method with silver NPs prepared using hot aqueous extract of T. orientalis. 3) Ag-SiO_2 NPs synthesize using sol-gel method with molar ratio $AgNO_3$: TEOS= 0.12. 4) Ag-SiO_2 NPs synthesize using sol-gel method with molar ratio $AgNO_3$: TEOS= 0.24.

The coloration that appeared in the nano composite is due to the silver ions reduction. Characteristic peaks from 390 to 420 nm correspond to the yellow colour of samples [24]. The increasing in the wavelengths is lead to decreasing in the grain size. These results have good agreement with the results obtained from XRD, AFM and SEM measurements.

Antibacterial activity of Ag-SiO_2 nanoparticles by agar well diffusion method

The results showed that the different size of inhibition zone depends on the kind of nanoparticles (nanogel and nanopowder) and the type of pathogenic bacteria as shown in Table 5. The nanogel samples showed an inhibition effect against *S. aureus* and *E. coli* bacteria than the nanopowder samples Fig. 10 b. The nanogel of sample 4 displayed the highest inhibition zone (24, 17) mm against both *E. coli* and *S. aureus* bacteria respectively. The nanogel samples (1, 2 and 3) showed similar inhibition effect (9.5, 10 and 9) mm

against *E. coli* bacteria respectively, while only sample 1 displayed an inhibition zone 9 mm against *S. aureus* bacteria. The nanopowder of sample 2 showed the highest inhibition zone 25 mm against *S. aureus* bacteria Fig. 10 a, while the nanopowder samples 1 and 4 showed the inhibition zone 12 and 15 mm against *S. aureus* bacteria. All the nanopowder samples showed no inhibition effect against *E. coli* bacteria. The nanoparticles type has an essential role in the inhibition effect against pathogenic bacteria. The nanogel can diffuse bacterial in the plate better than the nanopowder in addition the kind of the bacterial cell wall (Gram negative or positive) can play an important role by showing the effect of nanoparticles [25]. The results indicate that the smaller nanosilver particles are more active than larger ones because of their higher surface area [26].

Table 5: The effect of Ag-SiO_2 NPs on S. aureus and E. coli bacteria by using agar well diffusion method. 1) Ag-SiO_2 NPs that synthesize using sol-gel method with 10^{-3} M $AgNO_3$. 2) Ag-SiO_2 NPs produced using sol-gel method with silver NPs prepared using hot aqueous extract of T. orientalis. 3) Ag-SiO_2 NPs synthesize by using sol-gel method with molar ratio $AgNO_3$: TEOS= 0.12. 4) Ag-SiO_2 NPs synthesize by using sol gel method with molar ratio $AgNO_3$: TEOS= 0.24.

Bacterial species / Samples	*S. aureus* Inhibition zone (mm)		*E. coli* Inhibition zone (mm)	
	nanogel	**nanopowder**	**nanogel**	**nanopowder**
1	9	12	9.5	——
2	——	25	10	——
3	——	——	9	——
4	17	15	24	——

Well diameter for nanogel: 6mm
Well diameter for nanopowder: 8mm

(a) **(b)**

Fig. 10: (a) Inhibition zone for sample 2 (Ag-SiO_2 nanopowder) produced by using sol-gel method with silver NPs prepared by using hot aqueous extract of T. orientalis against S. aureus. (b) Inhibition zone for sample 4 (Ag-SiO_2 nanogel) synthesize using sol-gel method with molar ratio $AgNO_3$: TEOS= 0.24 against E. coli.

The effect of Ag-SiO_2 NPs on biofilm formation using microtiter plate method

From the results that shown in Table 6, the variation in biofilm values depends on the type of Ag-SiO_2 nanoparticles and microbial pathogens. All the types of Ag-SiO_2 NPs that synthesized by using both the chemical and green methods presented high inhibition effect against the entire microorganism compared with the control. The synthetic Ag-SiO_2 NPs in sample 3 had displayed the highest inhibition effect on Gram positive bacteria *S. aureus* compared with the control, while the less effect against the same bacteria was displayed by the Ag-SiO_2 NPs in sample 4 as shown in Fig. 11. The Ag-SiO_2 NPs in sample 1 shown the highest inhibition effect against the biofilm formation of *E. coli* bacteria, but Ag-SiO_2 NPs in sample 4 displayed the less effect against the same bacteria compared with the control. The value of high inhibition effect of Ag-SiO_2 NPs in sample 1 and 2 against biofilm formation of *S. aureus* bacteria was similar to each other, as well as for the high inhibition effect of Ag-SiO_2 NPs in sample 2 and 3 against biofilm formation of *E. coli* compared with the control.

Table 6: The effect of different Ag-SiO_2 NPs of biofilm formation for pathogenic bacteria. 1) Ag-SiO_2 NPs that synthesize using sol-gel method with 10^{-3} M $AgNO_3$. 2) Ag-SiO_2 NPs produced using sol-gel method with silver NPs prepared using hot aqueous extract of T. orientalis. 3) Ag-SiO_2 NPs synthesize using sol-gel method with molar ratio $AgNO_3$: TEOS= 0.12. 4) Ag-SiO_2 NPs synthesize using sol-gel method with molar ratio $AgNO_3$: TEOS= 0.24.

Bacterial species / Samples	*S. aureus*	*E. coli*
Control	**0.2773	*0. 2
1	0.0905	0.074
2	0.085	0.08
3	0.059	0.087
4	0.116	0.106

Standard deviation (S.D): 0.153
Cut-Off: 0.567
* moderate biofilm producer
** strong biofilm producer

Accordingly, isolates were classified as follows: O.D < 0.12 = no biofilm producer or weak biofilm producer, 0.12 < O.D ≤ 0.24 = moderate biofilm producer and 0.24 < O.D = strong biofilm producer (Magesh et al., 2013) [27].

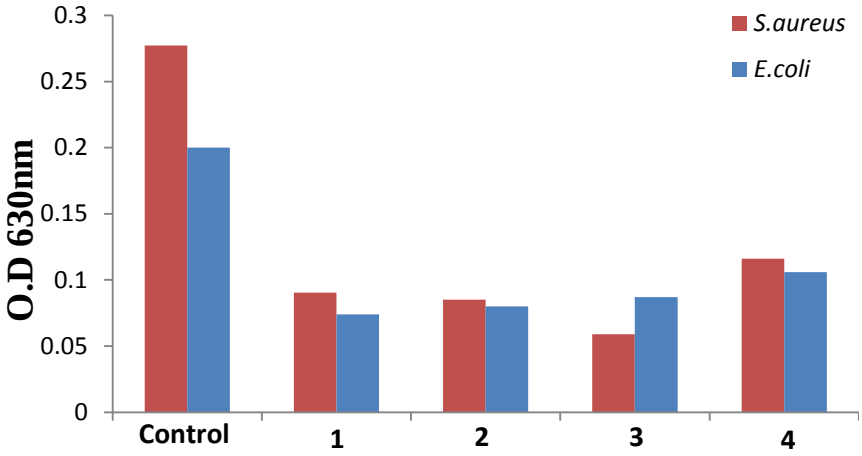

Fig. 11: The effect of different Ag-SiO_2 NPs on the (%) inhibition of biofilm formation for pathogenic bacteria. 1) Ag-SiO_2 NPs that synthesize using sol-gel method with 10^{-3} M $AgNO_3$. 2) Ag-SiO_2 NPs produced by using sol-gel method with silver NPs prepared by using hot aqueous extract of T. orientalis. 3) Ag-SiO_2 NPs synthesize using sol-gel method with molar ratio $AgNO_3$: TEOS= 0.12. 4) Ag-SiO_2 NPs synthesize using sol-gel method with molar ratio $AgNO_3$: TEOS= 0.24.

The effect of nanometals on inhibition of the biofilm formation is due to released that metal ions subsequently may bind with DNA molecules and lead to disordering of the helical structure by cross-linking within and between the nucleic acid strands and also disrupt the biochemical processes and protein denaturation and cause cell death [28, 29]. Another proposed mechanism is, there will be metal ions released from the nanoparticles that may attach to the negatively charged bacterial cell wall and rupture it, thereby leading to protein denaturation and cause cell death [28]. All the types of Ag-SiO_2 NPs showed high inhibition effect against the entire bacteria compared with the control. The Ag-SiO_2 NPs that synthesized had displayed the highest inhibition effect on gram positive (*S. aureus)* then gram negative bacteria (*E. coli).* Gram negative bacteria exhibit only a thin peptidoglycan layer between the cytoplasmic membrane and the outer membrane; in contrast, gram positive bacteria lack the outer membrane but have a peptidoglycan layer of about 30 nm thick [30].

Conclusions

The silica-silver NPs were prepared by using the sol-gel method with different preparations and concentrations. The crystalline structure of Ag-SiO_2 NPs that synthesized by using sol-gel method with silver NPs prepared by using hot aqueous extract of *T. orientalis* showed the path of the diffraction patterns. All the samples have a Face Center Cube (F.C.C.) back to silver nanoparticles submerged in the silica amorphous matrix and the average crystal size of sample 2 is 9.72 nm. Analysis of morphology using atomic force microscope (AFM) showed that the particle size was 74.09 nm. Silver-silica nanoparticles were characterized using a scanning electron microscopy (SEM) analysis and found to be a particle size of 20.154 nm. Silver-silica nanoparticles are highly stable and showed an inhibition effect against both Gram positive and negative bacteria.

Acknowledgment

The authors like to acknowledge the Central Enviromental Laboratory, Physics Department, College of

Science, University of Baghdad, and Physics Department, College of Women Science, University of Baghdad.

References

[1] P. Tippayawat, N. Phromviyo, P. Boueroy, A. Chompoosor: Peerj., 12 (2016) 1-15.
[2] A. Alkahlout: Ph.D. Thesis, Universidad des Saarlanders, (2006).
[3] P. Tatar, N. Kiraz, M. Asiltürk, F. Sayılkan, H. Sayılkan, E. Arpaç, Journal of Inorganic and Organometallic Polymers and Materials, 17, 3 (2007) 525-533.
[4] H. Wu, J. Huang, Yuejun Liu, Journal of Water and Health, 15, 3 (2017) 341-352.
[5] J. Cui, Y. Liang, Desong Yang, Yingliang Liu, Scientific Reports, 6 (2016) 1-10.
[6] L. Tang, J. Cheng, Nano Today, 8 (2013) 290-312.
[7] H. Zhang, J. A. Smith, V. Oyanedel-Craver, Water Res., 46 (2012) 691-699.
[8] J. Cui, J. Mater: Chem., 22 (2012) 8121-8126.
[9] K. A. Mauritz, R. M. Warren: Macromolecules, 22, 4 (1989) 1730-1734.
[10] K. Mezaal, M.SC. Thesis, Biochemical Engineering, Baghdad University, (2015).
[11] B. Pawar, D. S. Negi, International Journal of Pharma and Bio Sciences, Nanotechnology, 8, 2 (2017) 156-162.
[12] G. Sharma, A. R. Sharma, M. Kurian, R. Bhavesh, J. S. Nam, S. S. Lee, Digest Journal of Nanomaterials and Biostructures, 9, 1 (2014) 325-332.
[13] H. Hradecká, J. Matoušek, Ceramics – Silikáty, 54, 3 (2010) 219-224.
[14] J. H. Joa, P. Singha, J. Kima, C. Wanga, R. Mathiyalaganb, C. Jina, Yangab, D.C., Nan Med. Biotechnol. Int. J., 44, 6 (2015) 1-6.
[15] S. N. Goh, A. Fernandez, S. Z. Ang, W. Y. Lau: J. Biol. live Sci., 2, 13 (2013) 225-245.
[16] H. M. Abass, M. F. Ahmad, Diyala J. Agric. Sci., 6, 2 (2012) 27-38.
[17] I. K. Suh, H. Ohta, Y. Waseda, Journal of Materials Science, 23 (1988) 757-760.
[18] M. M. D. Lu, D. M. R. Silva, E. K. P. De, A. N Fajardo, Philippine e-Journal for Applied Research and Development, 5 (2015) 11-22.
[19] J. R. González-Castillo, E. Rodriguez, E. Jimenez-Villar, D. Rodríguez, I. Salomon-García, Gilberto F. de Sá, T. García-Fernández, D. B Almeida, C. L Cesar, R. Johnes, Juana C. Ibarra, Nanoscale Research Letters, 10, 399 (2015) 1-9.
[20] F. Kh. Abdul, M. Mazhar, M. R. Anwar and M. Taj, Applied Surface Science, 256 (2010) 2031-2037.
[21] S. Santra, United States, Patent Application Publication Santra, Orlando, FL, US., (2013) 1-20.
[22] Z. Li, A. Gu, Q. Zhou, Crystal Research and Technology, 44 (2009) 841-844.
[23] J. J. Mock, M. Barbic, D. R. Smith, D. A. Schultz, S. Schultz, Journal of Chemical Physics, 116 (2002) 6755-6759.
[24] M. Novotný, J. Matoušek, Ceramics − Silikáty 52, 2 (2008) 72-76.
[25] J. S. Thomas, D. Kahne, S. Walker, Journal Cold Spring Harbor Perspectives in Biology, 2, 5 (2010) 1-16.
[26] G. A. Sotiriou, S. E. Pratsinis, Environ. Sci. Technol., 44 (2010) 5649-5654.
[27] H Magesha, A. Kumara, A. Alama, Priyama, U. Sekarb, V. N. Sumantranc, R. Vaidyanathan, Indian Journal of Experimental Biology, 51 (2013) 764-772.
[28] H. R. Naika, K. Lingarajua, K. Manjunathb, D. Kumarc, G.

Nagarajuc, D. Sureshd, H. Nagabhushanae, J. Taibah Univ. Sci., 9, 1 (2015) 7-12.
[29] M. Sravanthi, D. M. Kumar, B. Usha, M. Ravichandra, M. M. Rao, K. P. Hemalatha, Biotechnol. Tech., 4, 8 (2016) 589-602.
[30] J. R. Morones, J. L. Elechiguerra, A. Camacho, K. Holt, J. B. Kouri, J. T. Ramírez, M. J. Yacaman, Nanotechnology, 16, 10 (2005) 2346-2353.